The Messinian salinity crisis: open problems and possible implications for Mediterranean petroleum systems

Marco Roveri[1*], Rocco Gennari[1], Stefano Lugli[2], Vinicio Manzi[1], Nicola Minelli[1], Matteo Reghizzi[1], Angelo Riva[3], Massimo E. Rossi[3] & B. Charlotte Schreiber[4]

[1]*Department of Physics and Earth Sciences, University of Parma, Parco Area delle Scienze 157/A, 43124, Parma, Italy*

[2]*Department of Chemical and Geological Sciences, University of Modena and Reggio Emilia, Via Campi 103, 41125, Modena, Italy*

[3]*Eni Upstream and Technical Services, Via Emilia 1, 20097 San Donato Milanese (Milano), Italy*

[4]*Department of Earth and Space Sciences, University of Washington, Seattle, Washington 98195, USA*

** Corresponding author (e-mail: marco.roveri@unipr.it)*

Abstract

A general agreement on what actually happened during the Messinian salinity crisis (MSC) has been reached in the minds of most geologists, but in the deepest settings of the Mediterranean basin the picture is still far from being finalized and several different scenarios for the crisis have been proposed, with different significant implications for hydrocarbon exploration. The currently accepted MSC paradigm - the "shallow-water deep-basin" model - implying high-amplitude sea-level oscillations (>1500 m) of the Mediterranean up to its desiccation, is usually considered as a fact. As a consequence, it is on this model that the implications of MSC events on Mediterranean petroleum systems are commonly based.

Actually, an alternative, deep-water, non-desiccated scenario of the MSC is possible; it i) implies the permanence of a large water body in the Mediterranean throughout the entire Messinian salinity crisis, but with strongly reduced Atlantic connections and ii) envisages a genetic link between Messinian erosion of Mediterranean margins and deep brine development.

In this work we focus on the strong implications for the assessment of petroleum systems of the Mediterranean and adjoining areas (*e.g.*, Black Sea basin) that can be based on such a non-desiccated MSC scenario. In particular, the near-full basin model delivers a more realistic definition of Messinian source rock generation and distribution, as well as of the magnitude of water unloading processes and their effects on hydrocarbon accumulation.

The Messinian salinity crisis of the Mediterranean: the paradigm

The term "Messinian salinity crisis" (MSC) refers to the largest and geologically most-rapid set of high-amplitude environmental changes undergone by the peri-Mediterranean area during the Neogene and possibly the entire Phanerozoic. The sedimentary record of this event involves complex feedbacks between geodynamics, climate and biota, and resulted in a stratigraphy which left an indelible signature in the post-Messinian evolution of the Mediterranean basin, also with important implications for hydrocarbon exploration. Up to now a general agreement on what actually happened during the MSC, particularly in the deepest settings of the Mediterranean basin, is still far from clear; consequently, several different scenarios of the crisis are available (see Roveri *et al.*, 2014a).

This lack of consensus is mainly due to the difficulty in establishing a general, comprehensive, high-resolution stratigraphic framework for the upper Messinian. In fact, in this interval, due to the lack of fossils and for being fully included into the C3r chron, the classical bio-magnetostratigraphic tools cannot be used (Hilgen *et al.*, 2007; Roveri *et al.*, 2014a). Furthermore, most data come from onshore successions, which formed in shallow (0-200 m water depth) or intermediate-depth (200-1000 m water depth) sub-basins, while the deepest Messinian settings, where the largest volume of MSC products accumulated, are buried below the present-day Mediterranean abyssal plains. These deep deposits are virtually unknown, due to the difficulties (both technical and economic) in getting data through scientific drillings or in accessing industry data. Moreover, since onshore and deep offshore Messinian successions are physically disconnected, a synthesis and common view of the MSC remain very difficult to obtain (Roveri *et al*., 2014a,c; Lofi *et al*., 2011).

As a consequence, due to the need for additional deep basin data, all the different scenarios so far proposed should be considered as *theories* in need to be proven. However, the "shallow-water deep-basin" (SWDB - Hsü *et al.*, 1973) with its high-amplitude sea-level oscillations (>1500 m) up to its

desiccation, is the current MSC paradigm (Roveri & Manzi, 2006; Roveri *et al.*, 2014b). This model is usually considered as a *fact*, with obvious implications in many related fields including hydrocarbon exploration, but such a view could lead to possible misinterpretation.

This model has undergone some modifications through time, all implying that at a certain point the Mediterranean desiccated almost completely and its slopes underwent a phase of subaerial exposure and vigorous erosion related to the rejuvenation of an entire fluvial drainage system (Lofi *et al.*, 2005; Ryan, 2009; Bache *et al.*, 2012). This phase of generalized exposure would have led to the formation of an erosional surface (Messinian erosional surface – MES), which is one of the main stratigraphic features in both onshore and offshore records and a key one for their correlation. The rapid water loading/unloading events would have caused significant pressure release and catastrophic fluid expulsion phenomena (Ryan et al., 1978; Bertoni *et al.*, 2013; Sacleux et al., 2013; Bertoni & Cartwright, 2015) with great impact on pre-existing hydrocarbon migration and preservation.

We think that an alternative scenario, implying the permanence of a large and deep-water body connected with the Atlantic Ocean throughout the MSC (Schmalz, 1969; Roveri *et al.*, 2014b), is not only possible but even more likely. In this paper we also discuss the more general implications of our new scenario for petroleum systems.

An alternative scenario: stratigraphic framework

Our scenario is based on a recently established chronology of the main MSC events mainly built on onshore data (Krijgsman *et al.*, 1999; Hilgen *et al.*, 2007; Manzi *et al*., 2013) , which includes both outcrop and subsurface data. A major consensus has been reached on this stratigraphic framework, which includes three evolutionary stages (Clauzon *et al*., 2006; CIESM, 2008; Roveri *et al.*, 2014a; Fig. 1), each of them characterized by a particular evaporite association recording significant

hydrological changes in the Mediterranean basin. The latter are well documented by the $^{87}Sr/^{86}Sr$ Mediterranean curve (Fig. 1), which shows a significant, stepwise detachment from the global ocean curve during the MSC, suggesting a progressive hydrological isolation and/or an increase of the relative proportion of continental waters over the ocean ones (see Flecker *et al.*, 2002; Roveri *et al.*, 2014c). Each one of the three stages of the crisis shows a distinct range of $^{87}Sr/^{86}Sr$ values: >0.708900 for stage 1, between 0.708800 and 0.708900 for stage 2 and <0.708800 for stage 3. In the following section we briefly summarize the main characteristics of each MSC stage.

MSC onset and stage 1 (5.97-5.60 Ma)

The onset of the MSC occurred synchronously at 5.97 Ma (Manzi *et al*., 2013), *i.e.* well after the base of the Messinian stage (7.246 Ma), following a long phase of progressive reduction of Atlantic connections and consequent restriction of Mediterranean circulation and water column stratification witnessed by the widespread cyclical deposition in deep marine settings of organic and opal-rich sediments (pre-MSC stage; *e.g.*, Tripoli Fm. of Sicily, Hilgen & Krijgsman, 1999).

The onset of the crisis is not necessarily coincident with the base of the lowermost evaporite bed, as sometimes erroneously envisaged in the literature (see for example Ochoa *et al*., 2015) but by a dramatic decrease of normal marine biota followed by their disappearance (Manzi *et al*., 2007; 2013; 2015). In fact, while the biological record of the onset of the crisis is synchronous throughout the Mediterranean basin and at any depth, the onset of the bottom-grown evaporites of the stage 1 (selenite gypsum of the Primary Lower Gypsum unit - PLG) is diachronous (Roveri et al., 2014a; Manzi et al., 2016). PLG evaporites started to form since 5.97 Ma only in shallow water, semiclosed, silled sub-basins developed along the Mediterranean continental margins (Lugli *et al*., 2010), whereas moving to deeper setting the onset of the PLG is progressively younger (Lugli et al., 2010; Dela Pierre et al., 2011; Roveri et al., 2014a). The water depth limiting the deposition of the bottom-grown gypsum (< 200 m, including areas beyond the shelf break) is suggested by the common occurrence of photosynthetic microorganisms communities trapped within primary

gypsum crystals (mainly cyanobacteria; Panieri *et al.*, 2010). MSC onshore records clearly show that in deeper and/or ~~not~~ unsilled sub-basins, evaporite-free deposits accumulated, mainly consisting of organic-rich shales and dolostones barren of normal marine fossils (Manzi et al., 2007; Lugli *et al*., 2010; Dela Pierre *et al.*, 2011; Ghielmi et al., 2013; Rossi et al., 2015).

Evaporite deposition was modulated by precession-controlled climatic oscillations inducing changes of the Mediterranean hydrological budget (Vai, 1997; Krijgsman *et al.*, 1999; Hilgen *et al*., 2007). Up to 16 gypsum-shale couplets recording dry-wet precessional cycles formed in stage 1, allowing the end of this phase to be dated at 5.60 Ma (Krijgsman *et al*., 1999; Roveri *et al.*, 2014a). The lithology of these cycles show an impressive similarity in terms of types of gypsum sedimentary facies, stacking patterns and overall trend, permitting pan-Mediterranean bed-by-bed correlation (Lugli *et al.*, 2010). The gypsum in these beds formed subaqueously; each precessional evaporitic cycle is characterized by a facies sequence recording a progressive increase in brine saturation, followed by a phase of relative dilution (Roveri et al., 2008a); it is worth noting that evidences of subaerial exposure and/or erosion are not observed within these cycles but only at the top of the PLG unit.

This PLG unit may locally consist of less than 16 gypsum cycles, due to the absence of the basal members (replaced by their laterally equivalent evaporite-free deposits; Manzi *et al.*, 2007; Dela Pierre *et al*., 2011; Gennari *et al.*, 2013) or because of erosion and resedimentation during the subsequent stage 2 (Roveri *et al*., 2001; 2014; Manzi *et al*., 2005).

~~Differently to~~ Unlike what is claimed by some authors (e.g., Ochoa et al., 2015), where outcrop observations and complete subsurface data (seismics and boreholes) are available, it has been documented that the PLG evaporites are absent in deep-water and/or unsilled settings during the MSC stage 1 (Manzi et al., 2007; Lugli *et al*., 2010; Dela Pierre *et al.*, 2011; Ghielmi et al., 2013; Rossi et al., 2015). Two different models have been proposed so far to explain this fact.

Lugli *et al*. (2010) suggest that bottom-grown gypsum only developed in shallow (< 200 m), silled sub-basins acting as bottom brine traps; De Lange & Krijgsman (2010), suggest that a sill is

not necessary and that the main controlling factor is the rate of sulphate consumption due to degradation of organic matter which, in deep water below 200 m, would be greater than the supply rate of sulphate, thus hampering gypsum precipitation and preservation. ~~Thus,~~ Both models recognize the absence of primary evaporites of the first stage in deep-water settings and this fact is a fundamental observation for the correlation of deposits from shallow to deep parts of the basin.

Stage 2 (5.60-5.54 Ma)

The second stage of the crisis is characterized by a period of strong erosion of Mediterranean continental margins (MES) and by the concurrent deposition of huge volumes of highly-soluble primary evaporites (halite and K-Mg salts) as well as of resedimented PLG evaporites (i.e. as a clastic facies) in deeper sub-basins (Apennines, Sicily, Calabria, Tuscany, Cyprus). The resulting unit observed in onshore successions has been named Resedimented Lower Gypsum (RLG) and shows very rapid and significant lateral changes in terms of lithology and thickness, which is also related to tectonic activity affecting several Mediterranean areas in this stage. The clastic component of RLG unit mainly consists of gypsum turbidites, giant PLG olistoliths (Roveri *et al.*, 2001, 2008b; Manzi *et al.,* 2005) and microbially-derived brecciated limestones (*i.e.* the Calcare di Base of Sicily; Manzi *et al*., 2011); locally the RLG unit may mainly consist of terrigenous sediments (*i.e.* turbiditic sandstones of the Apennine~~s~~ foreland system depocenters – the Laga p.p. and Fusignano Formations; Roveri *et al.*, 2001; Manzi *et al*., 2005; Rossi *et al.*, 2015). This stage, which is considered the acme of the crisis, encompasses a very short time window, according to cyclostratigraphic considerations based on stage 1 (Roveri & Manzi 2006) and stage 3 cyclic patterns (Manzi *et al*., 2009). Thus the RLG unit would end at 5.54 Ma spanning no more than 60 ka.

Subaerial erosion of stage 1 evaporites (PLG) is commonly observed in onshore successions, suggesting a relative base-level fall whose amplitude, however, cannot be clearly defined (see Lugli

et al., 2013; 2015; Roveri *et al*., 2014b). Onshore, the MES can be traced downbasin in deeper settings at the base of the RLG unit (Manzi *et al.*, 2005; 2007). It is worth noting that in such settings the deep water equivalent of PLG evaporites do not show evidence of subaerial exposure; in some places these deposits are eroded at the top and only partially preserved, thus suggesting subaqueous erosional processes.

Stage 3 (5.54-5.33 Ma)

The last stage of the MSC is probably the most enigmatic phase. Onshore successions consist of both shallow and relatively deeper water deposits. Sr isotope data (<0.708800) and fossils (mollusks and ostracods) suggest that surface waters underwent a significant dilution with the development of brackish environments throughout the Mediterranean. Deeper successions are usually barren of fossils, thus hampering palaeoenvironmental reconstructions. Despite this general signal of more diluted waters, primary evaporites (sulfates) are formed also in this stage, but only in the southern and easternmost sectors of the Mediterranean (e.g., Sicily, Calabria, Cyprus). These evaporites, named Upper Gypsum (UG) bear some lithologic similarities with stage 1 PLG evaporites, but can be easily distinguished based on their facies characteristics and particularly on their Sr isotope values (Manzi *et al.*, 2009). Like the PLG, the UG unit has a well-developed cyclical pattern induced by precession, which allows its accurate chronostratigraphic calibration. Stage 3 can be subdivided into substages 3.1 and 3.2, based on the sudden increase of terrigenous sediment input at around 5.42 Ma, especially in the northern and western Mediterranean sectors. Substage 3.2 is also characterized by the greatest development and diffusion of the inclusion of Lagomare faunal assemblages, which have been classically considered to derive from the Paratethys (e.g. Orszag-Sperber, 2006; Roveri et al., 2008a). In this low-salinity environment, some evidence of the permanence of the Atlantic connections is given by the occurrence of marine fish (Carnevale *et al*., 2008) and alkenons (Mezger *et al*., 2012). The return to normal marine conditions is sudden

189 and marks the base of the Zanclean at 5.33 Ma, usually interpreted as related to a catastrophic re-
190 opening of the Atlantic connections.

191 **Seismic and well log expression of evaporitic units**

192 When its 16 lithological cycles are largely preserved, the PLG unit may attain a total thickness
193 ranging between 100 and 300 meters (Lugli et al., 2010), typically around 150-200 m in the best
194 outcrops of the Apennines, Sicily and southern Spain. This unit does not have a peculiar seismic
195 facies allowing to distinguish it from the evaporitic units of the other MSC stages, especially where
196 only commercial, low-resolution seismic profiles are available. In this case, it appears as a thin
197 seismic unit consisting of 1-2 parallel, high amplitude reflectors, similar to the RLG and UG units,
198 where the latter are thinner. However, the PLG unit can be well identified in well logs due to its
199 peculiar blocky pattern, as documented in many offshore and onshore boreholes (Roveri et al, 2005;
200 Lugli et al., 2010; Rossi et al., 2015). Where high-resolution seismic profiles are available, PLG
201 evaporites appear as a horizontal bedded unit (BU of Lofi et al., 2011) with a conformable base and
202 an erosional top (e.g. the MES; see Maillard et al., 2014; Driussi et al., 2015); the erosional vs. non-
203 erosional character of the bounding surfaces is probably the most useful criteria for distinguishing it
204 from other evaporite-bearing units (i.e. the suggested equivalents of RLG and UG units,
205 respectively the MU and UU units of Lofi et al., 2011). RLG, in particular, is usually thicker (up to
206 2 km in the deepest Mediterranean basins) and mainly consisting of halite, thus appearing as an
207 acoustically transparent seismic unit; locally, the RLG unit may include chaotic seismic facies
208 related to slump and/or debris flow deposits. Its base, the MES, is commonly unconformable at
209 margins and becomes conformable in the basin center.
210

211 **The onshore lesson: clues for shallow to deep correlations**

212 This three-stage Messinian stratigraphic framework is based on the onshore record of the MSC but

has a large potential for also being applied to deep offshore successions because of its robust physical stratigraphic architecture, constrained by key surfaces and time lines (*e.g.*, MES, Zanclean base) that can be easily recognized from available seismic and borehole data, allowing a sequence-stratigraphic approach (Roveri *et al*., 2008c; Rossi *et al.*, 2015). The three stages of the model are characterized by distinctive Sr isotope values that can be easily obtained analyzing the evaporite rocks and the fossils from cores or cuttings. A first attempt of suggesting an onshore-offshore correlation has been provided by Roveri *et al.* (2014c; Fig. 2) based on the recognition that onshore successions also include intermediate-depth (up to 1,000 m) depocenters showing continuous subaqueous deposition. These relatively deep settings are the key stratigraphic link between the shallow and the deep basin records.

According to this correlation, a possibility exists that the largest part of the evaporitic deposits lying in the deepest basins could have formed during MSC stage 2. The evaporitic unit in the western Mediterranean and in the Ionian basin is a tripartite seismic unit (the famous "Messinian trilogy"); the three seismic units (LU, Lower Unit; MU, Mobile Unit; UU, Upper Unit; Lofi et al., 2011) have been classically considered to be the offshore equivalent, from the bottom to the top, of the Lower Gypsum (*i.e.* the PLG), of the Sicilian salt and of the Upper Gypsum. In the Levantine Basin the evaporitic unit is not tripartite and only the MU is recognized (Lofi et al., 2011).

Actually the MES, marking the boundary between stages 1 and 2, can be traced downbasin to deep offshore areas, where it corresponds to the basal surface of the deep canyons (Lugli *et al.*, 2013) that possibly continued into the erosional features imaged at the base of the deep Levantine evaporites (Bertoni and Cartwright, 2007). The MES also represents a pervasive erosional surface of the Mediterranean slopes that can be followed in the deeper basins (BES; Lofi et al., 2011) and that progressively smooths out in the basin plain settings becoming a correlative conformity (BS; Lofi et al., 2011) marking the base of the Lower Evaporites (Lower Unit; Lofi *et al.*, 2005; 2011)**.**

Because of these characteristics the MSC stages 1 and 3 would be represented respectively by: i) a thin, evaporite-free layer below the base of the Lower Evaporites; ii) a relatively thin unit, mostly

below seismic resolution, composed of shales with minor evaporites laying above the Mobile unit. As for the uppermost evaporites of the MU recovered from the DSDP-ODP cruises, Sr isotopes signature suggest they still belong to the MSC stage 2 (Roveri *et al.,* 2014c),.

An alternative scenario: erosion and deposition in a non-desiccated deep Mediterranean basin

The shallow water-deep basin model (SWDB) is mainly based on: 1) the interpretation of the erosional features of the margins as due to mostly subaerial processes, and 2) the supposed shallow-water to subaerial nature of the deep evaporites. As for the second point, recent studies (Hardie & Lowenstein, 2004; Lugli *et al.*, 2015) have demonstrated that the evaporites at the top of the MU do not show evidence for subaerial exposure and could have precipitated at any water depth. As for the first point, it was possible to document that only the~~ir~~ shallower parts of the onshore successions underwent subaerial erosion during stage 2, while the intermediate-depth depocenters experienced continuous subaqueous deposition throughout the crisis and/or subaqueous erosion mainly by gravity flows and related slope failure processes.

Starting from these considerations, Roveri et al. (2014) suggest a genetic link between the deposition of salt in the deepest basins and the erosion along the basin slopes due to the downslope flow of hypersaline, dense waters which led to the formation of deep-water brines. This process is similar to the present-day cascading of dense shelf waters along the Mediterranean margins (Canals *et al*., 2006); together with sediment gravity flows (i.e. turbidites and hyperpycnal fluvial floods) these processes work together to shape submarine slopes and to cut gullies and canyons (Roveri *et al*., 2014b). We infer that the Messinian slopes were profoundly reshaped during the MSC, and particularly during stage 2, by forming new erosional features or by rejuvenating pre-existing ones, as documented along both the western (Lofi & Berné, 2008) and eastern (Lugli *et al.,* 2013) Mediterranean margins. However, the MES was not generated exclusively by subaqueous processes, since a moderate relative sea-level fall, ranging in amplitude between 200 m (Roveri et

al., 2014b) and 550 m (Rossi et al., 2015) also promoted the subaerial exposure and erosion of the basin margins. It follows that the MES is a polygenic erosional surface with both subaerial and subaqueous tracts, mainly developed during the peak of the MSC and commonly superimposed on older features. Stage 2 was then characterized by two high-amplitude glacial episodes (TG12 and TG14; Fig. 1) and by an acceleration of active tectonic processes along the entire Africa-Eurasian margin, as clearly shown by the angular unconformity commonly associated with the MES. Thus, in our opinion, a number of geodynamic and climatic causes acted simultaneously to modify the water and the atmospheric circulation within the Mediterranean during the Messinian. These causes were likely linked to complex feedback mechanisms leading to an extreme amplification of processes still acting today along the Mediterranean margins. The Black Sea slopes are characterized by a widespread erosional surface of Messinian age whose origin has been usually interpreted as related to desiccation, similarly to the Mediterranean (Hsü & Giovanoli, 1979); however, Messinian evaporites are absent in the Black Sea (Tari et al., this volume). As occurs in modern time (Flood et al., 2008), we argue that during Messinian cascading of hypersaline, dense waters, together with sediment gravity flows, could have produced the Black Sea erosional surface as well. But in a different way from the Mediterranean, Black Sea deep brines might not have not reached high saturation values, thus explaining the lack of evaporitic deposits.

In our model the Mediterranean was a persistent water body characterized by reduced connections with the Atlantic, and by a hydrological budget controlled by regional climate oscillations and by exchanges with the freshwater reservoir of the Paratethys basin(s) (Krijgsman *et al.,* 2010). This general setting could well explain also the last portion of the salinity crisis, which was considered to be characterized by an empty Mediterranean basin with several isolated freshwater or brackish lakes. According to our model, this phase (MSC stage 3) was instead likely characterized by an overall positive hydrological budget and a high base-level, punctuated by cyclical episodes of relative base level fall (Roveri et al., 2008a; Manzi et al., 2009; Roveri et al., 2014a-c; Rossi et al., 2015). Also in this late stage the Mediterranean was a single, permanent water body, as suggested

by the ostracod assemblages (Stoica *et al.*, 2016) and uniform Sr isotope values (Roveri *et al.*, 2014a-c).

An alternative scenario: implications for hydrocarbon exploration

The Messinian successions are characterized by an extreme lithological variability expressed in a complex stratigraphy which resulted in a diverse array of potential source rocks, reservoirs and seals. For these reasons, besides their own potential as a petroleum system, the Messinian sediments also played a substantial role for the other Mediterranean petroleum systems, especially for the pre-Messinian ones (see Pawlewicz, 2004; Belopolskyi *et al.*, 2012; Al-Belushi *et al.*, 2013; Bertoni *et al.*, 2015). We think that our chronostratigraphic framework and sequence-stratigraphic approach may help to better identify and characterize those potentials in a coherent scenario.

Here we will focus on two elements directly deriving from our model that should be considered for their potential implications for hydrocarbon exploration: the Messinian source rocks and the effects of base-level changes throughout the crisis.

The Messinian source rocks

Source rocks originate from zones of high organic productivity and where organic-rich sediments are deposited in a low-oxygen environment allowing their preservation. During the Messinian the intermediate and deep-water settings were characterized by water stratification throughout the salinity crisis and even before, due to restricted exchanges with the Atlantic, which eventually led to the formation of deep brines; this resulted in the development of conditions favoring the accumulation and preservation of organic-rich deposits.

The source rock potential of MSC deposits has been documented in several areas: the Chelif Basin (Northern Algeria; Arab et al., 2015), the Prinos-Kavala Basin (Northern Aegean; Kiomourtzi et al., 2008), the island of Zakynthos and the Hellenic Trench (Greece; Maravelis et al., 2013; 2015), and

314 the Northern Apennines (Manzi et al., 2007). However, a full knowledge of the Messinian source
315 rocks is lacking, mainly due to the difficulty in organizing the available scattered data and
316 observations into a comprehensive and detailed stratigraphic framework.

317 In this respect our MSC scenario offers some clues for a better definition of the source rock
318 potential. We show here a first attempt to systematically organize the available data concerning
319 organic matter in order to assess their areal and temporal distribution and characteristics. We
320 collected Rock-Eval Pyrolisis data (Espitalié et al., 1977) from the literature, also including a set of
321 unpublished data, mainly from Northern Italy and Sicily (Fig. 3a). After age re-calibration of the
322 available samples, we plotted the S2-TOC (Fig. 3b-f) and the Hydrogen and Oxygen Index (HI, OI;
323 Fig. 3j-k) values of sediments belonging to the same stage from different areas. The compilation of
324 these organic matter data into our three-stage~~s~~ chronostratigraphic model provides some revealing
325 trends and features (see below).

326 Substantially every sample considered in this work is immature (Tmax <435°C), particularly those
327 collected in exposed successions; however, local and regional-scale geological reconstructions
328 document that in the main depocenters, Messinian organic-rich units may have reached burial
329 depths sufficient for the attainment of thermal maturity.
330 S2-TOC values (Fig. 3b-f) provide an estimate of the petroleum potential, and show that most stage
331 1 and 2 values plot in an overall good potential field. Conversely, MSC Stage 3 is generally
332 characterized by reduced organic carbon content and S2 values.
333 The different kerogen types were defined mainly based on the Hydrogen Index; in Fig. 3e-k we
334 display modified Van Krevelen diagrams for samples with TOC > 0.5 % (note that roughly ~~a~~ 20%
335 of these are not represented because ~~since~~ no S3 data were available). HI values show that organic
336 matter of deep-water pre-MSC sediments and stage 1 range between type II and II-III kerogens
337 (*sensu* Peters and Cassa, 1994); stage 2 organic matter plots between kerogen types II and I;
338 conversely, stage 3 records a progressive shift towards kerogens types III-IV, possibly representing

339 an increased influence of continental input in the latest stage of the MSC (see also the organic
340 matter composition of the Northern Apennines Messinian units in figure 4).

341 Our results show that the deep-water equivalent of the evaporite deposits of stage 1 have a very
342 good source rock potential, also considering that this unit, where it is preserved below the
343 resedimented evaporite deposits, may have thicknesses in the order of several tens of meters in
344 outcrop (≈ 60 m in the Northern Apennines; Fanantello borehole, Manzi *et al*., 2007), up to 400
345 meters in the subsurface (Po Plain foredeep basin; Rossi et al., 2015). Furthermore, in the deeper
346 basins, where anhydrite derived from the transformation of clastic gypsum due to lithostatic loading
347 (Manzi *et al.*, 2005; Lugli et al., 2013) may represent an efficient early seal, preventing migration of
348 Messinian hydrocarbons.

349 In this scenario, the close association in deep settings of the potential source rock (*i.e.* deep water
350 stages 1 and 2 deposits) directly overlain by or interlayered with clastic evaporite deposits may be
351 of great importance for the reconstruction of hydrocarbon migration pathways and for the
352 recognition of potential reservoirs. In this respect it is worth noting that frequently (e.g., Northern
353 Apennines and Sicily), large-scale zones of sulphur mineralization are associated with RLG clastic
354 evaporites. Sulphur formed after bacterial sulphate reduction of Messinian evaporites favored by
355 hydrocarbon migration and leading to the transformation of the parent rock into sulphur-bearing
356 limestone (Dessau et al., 1962; Manzi et al., 2011). Although hydrocarbons involved in these
357 processes may be older sources, the close association of sulphate and organic-rich rocks may point
358 to a Messinian source rock.

359

360 ***Amplitude of Mediterranean base-level changes***

361 In the scenario of Roveri et al. (2014b) the amplitude of base-level changes during the salinity crisis
362 was much less pronounced than usually envisaged; we think that the Mediterranean Sea

363 experienced only a moderate relative base-level fall (Christeleit et al., 2015) and that desiccation, as
364 well as a catastrophic refill (Hsü et al., 1973), did not occur. The lower slopes and the deep-water
365 settings did not undergo subaerial exposure and erosion. It follows that the organic matter in the
366 pre-MSC and in the stage 1 deposits was far better preserved than expected for a complete basin
367 desiccation.

368 Besides these more obvious aspects, the desiccation scenario implies rapid and massive water
369 loading/unloading in the order of thousands of meters (Ryan et al., 1978; Govers *et al.*, 2009;
370 Sacleaux et al., 2013). These changes and their isostatic effects would cause overpressure and
371 catastrophic fluid expulsions even through the thick Messinian evaporitic unit, that is usually
372 considered an ideal seal (Bertoni & Cartwright, 2015). Another aspect would be the degradation
373 and/or remigrations of pre-existing hydrocarbons (Al-Belushi *et al.*, 2013; Iadanza *et al.*, 2015) with
374 important implications for assessing the overall quality of Mediterranean petroleum systems. In our
375 model, the magnitude of these processes would be considerably lower, translating to a significantly
376 lower exploration risk for pre-Messinian targets (cf. the Black Sea, Tari et al., this volume).

377

378 **Conclusions**

379 Far from being a "fact," as commonly considered, the desiccation model of the Messinian salinity
380 crisis is only one of the several possible scenarios. We suggest that an alternative, deep-water, non-
381 desiccated model for the MSC is not only possible, but also even more likely. This model has
382 several important implications for the assessment of the Mediterranean petroleum systems, as well
383 as of the adjoining area (e.g. Black Sea; Tari et al., this volume). We think that the impact of the
384 model for source rock generation and distribution, as well as for the effects of water unloading for
385 breaching pre-existing hydrocarbon accumulations, should be carefully considered and evaluated.
386 Our new data and a re-consideration of all available data suggests that the pre-salinity crisis

sediments and the stage 1 source rock have a greater potential than previously thought. In addition, the stage 2 resedimented deposits may provide an excellent seal especially at deep Mediterranean settings.

The onshore and offshore perspectives of the MSC will be reconciled only when deep drillings will hopefully reach the pre-salt unit and core data will be made available to the scientific community especially from sediments on the ocean floor of the Mediterranean. This obviously needs a great joint effort between academia and industry.

Acknowledgments

The organic geochemistry data and their petroleum geology implications derive in part from the results of a collaborative R&D project between ENI and the Universities of Parma and Modena-Reggio Emilia. U. Biffi and G. Caccialanza (ENI upstream and technical services) are gratefully acknowledged for their valuable contribute in processing the data and discussing their interpretation.

403

404 **References**

405 Al-Belushi, A.N., Fraser, A., Allen, P.A. & Jackson, C.A. 2013. Quantifying the uplift magnitude
406 caused by the Messinian Salinity Crisis and its impact on the Eastern Mediterranean Petroleum
407 Systems. AAPG Search and Discovery #90161.

408

409 Arab, M., Bracène, R., Roure F., Zazoun, R.S., Mahdjoub, Y. & Badji, R. 2015. Source rocks and
410 related petroleum systems of the Chelif Basin (western Tellian domain, north Algeria). *Marine and*
411 *Petroleum Geology*, **64**, 363-385.

412

413 Bache, F., Popescu, S.-M., Rabineau, M., Gorini, C., Suc, J.-P., Clauzon, G., Olivet, J.-L., Rubino,
414 J.-L. & others 2012. A two step process for the reflooding of the Mediterranean after the Messinian
415 salinity crisis. *Basin Research*, **24**(2), 125–153.

416

417 Belopolsky, A., Tari, G., Craig & J., Iliffe, J., 2012. New and emerging plays in the Eastern
418 Mediterranean: an introduction. *Petroleum Geosciences,* **18**, 371–372.

419

420 Bertoni, C., Cartwright, J. & Hermanrud, C. 2013. Evidence for large-scale methane venting due to
421 rapid drawdown of sea level during the Messinian Salinity Crisis. *Geology*, **41**, 371-374.

422

423 Bertoni, C. & Cartwright, J. 2015. Messinian evaporites and fluid flow. *Marine and Petroleum*
424 *Geology*, available online.

425

426 Canals, M., Puig, P., Durrieu de Madron, X., Heussner, S., Palanques, A. & Fabres, J. 2006.
427 Flushing submarine canyons. *Natur*e, **444**, 354–357.

Carnevale, G., Longinelli, A., Caputo, D., Barbieri, M. & Landini,W. 2008. Did the Mediterranean reflooding preceded theMio-Pliocene boundary? Paleontological and geochemical evidence from upper Messinian sequences of Tuscany, Italy. *Palaeogeography, Palaeoclimatology, Palaeoecology* **257**, 81–105.

Christeleit, E. C., Brandon, M. T., & Zhuang, G. 2015. Evidence for deep-water deposition of abyssal Mediterranean evaporites during the Messinian salinity crisis. *Earth and Planetary Science Letters*, **427**, 226-235.

CIESM 2008. The Messinian salinity crisis from Mega-deposits to Microbiology. A consensus report. *CIESM Workshop Monograph*, **33**.

Clauzon, G., Suc, J.-P., Gautier, F., Berger, A. & Loutre, M.F. 1996. Alternate interpretation of the Messinian salinity crisis: Controversy resolved? *Geology*, **24**(4), 363–366.

De Lange, G.J. & Krijgsman, W., 2010. Messinian salinity crisis: a novel unifying shallow gypsum/deep dolomite formation mechanism. *Marine Geology* **275**, 273–277.

Dela Pierre, F., Bernardi, E., Cavagna, S., Clari, P., Gennari, R., Irace, A., Lozar, F., Lugli, S., Manzi, V., Natalicchio, M., Roveri, M. & Violanti, D. 2011. The record of the Messinian salinity crisis in the Tertiary Piedmont Basin (NW Italy): the Alba section revisited. *Palaeogeography, Palaeoclimatology, Palaeoecology,* **310**, 238–255.

Deroo, G., Herbin, J.P. & Roucaché, J. 1978. Organic geochemistry of some Neogene cores from sites 374, 375, 377 and 378: Leg 42A, eastern Mediterranean sea. *In:* Hsü, K.J., Montadert, L.,

454 Bernoulli, D., Cita, M.B., Erikson, A., Garrison, R. et al. (eds) *Initial reports of the Deep Sea*
455 *Drilling Project*, **42**, 465-472, http://doi.org/10.2973/dsdp.proc.42-1.113-3.1978
456
457 Dessau, G., Jensen, M.L. & Nakai, N. 1962. Geology and isotopic studies of Sicilian sulphur
458 deposits. *Economic Geology*, **57**, 410-438.
459
460 Espitalie, J., M. Madec, B. Tissot, J. J. Mennig & Leplat, P. 1977. Source rock characterization
461 method for petroleum exploration. In: *Proceedings of the Ninth Offshore Technology Conference*,
462 Houston, **3**, 439-448.
463
464 Flecker, R., de Villiers, S. & Ellam, R.M. 2002. Modelling the effect of evaporation on the salinity–
465 $^{87}Sr/^{86}Sr$ relationship in modern and ancient marginal-marine systems: the Mediterranean Messinian
466 Salinity Crisis. *Earth and Planetary Science Letters*, **203**, 221–233.
467
468 Flood, R. D., Hiscott, R. N., & Aksu, A. E. 2009. Morphology and evolution of an anastomosed
469 channel network where saline underflow enters the Black Sea. *Sedimentology*, **56**, 807–839.
470
471 Ghielmi, M., Minervini, M., Nini, C., Rogledi, S. & Rossi, M. 2013. Late MioceneeMiddle
472 Pleistocene sequences in the Po Plain-Northern Adriatic Sea (Italy): the stratigraphic record of
473 modification phases affecting a complex foreland basin. *Marine Petroleum Geology*, **42**, 50-81.
474
475 Govers, R., Meijer & P. Krijgsman, W**.** 2009, Regional isostatic response to Messinian Salinity
476 Crisis events. *Tectonophysics*, **463**, 109-129.
477
478 Guido, A., Jacob, J., Gautret, P., Laggoun-Défarge, F., Mastandrea, A. & Russo, F. (2007),
479 Molecular fossils and other organic markers as palaeoenvironmental indicators of the Messinian

480 Calcare di Base Formation: normal versus stressed marine deposition (Rossano Basin, northern
481 Calabria, Italy). *Palaeogeography, Palaeoclimatology, Palaeoecology*, **255** (3-4), 265-283.
482
483 Hardie, L.A. & Lowenstein, T.K. 2004. Did the Mediterranean Sea dry out during the Miocene? A
484 reassessment of the evaporite evidence from DSDP Legs 13 and 42A cores. *Journal of Sedimentary*
485 *Research*, **74**, 453–461.
486
487 Hilgen, F.J., Kuiper, K., Krijgsman, W., Snel, E. & Van Der Laan, E. 2007. Astronomical tuning as
488 the basis for high resolution chronostratigraphy: the intricate history of the Messinian Salinity
489 Crisis. *Stratigraphy*, **4**, 231–238.
490
491 Hsü, K.J., Ryan, W.B.F. & Cita, M.B. 1973. Late Miocene desiccation of the Mediterranean.
492 *Nature*, **242**, 240–244.
493
494 Iadanza, A., Sampalmieri, G. & Cipollari, P. 2015. Deep-seated hydrocarbons in the seep
495 "Brecciated Limestones" of the Maiella area (Adriatic foreland basin): Evaporitic sealing and oil re-
496 mobilization effects linked to the drawdown of the Messinian Salinity Crisis. *Marine and*
497 *Petroleum Geology*, **66**, 177-191.
498
499 Krijgsman, W., Hilgen, F. J., Raffi, I., Sierro, F.J. & Wilson, D.S. 1999. Chronology, causes and
500 progression of the Mediterranean salinity crisis. *Natur*e, **400**, 652–655.
501
502 Krijgsman, W., Stoica, M., Vasiliev, I. & Popov, V.V. 2010. Rise and fall of the Paratethys Sea
503 during the Messinian Salinity Crisis. *Earth Planetary Science Letters*, **290**, 183–191.
504
505 Kiomourtzi, P., Pasadakis, N. & Zelilidis, A. 2008. Source Rock and Depositional Environment

506 Study of Three Hydrocarbon Fields in Prinos-Kavala Basin (North Aegean). *The Open Petroleum*
507 *Engineering Journal*, **1**, 16-29.
508
509 Lofi, J., Déverchére, J., Gaullier, V, Gillet, H., Guennoc, P., Gorini, C., Loncke, L., Maillard, A.,
510 Sage, F. & Thinon, I. 2011. Seismic atlas of the Messinian salinity crisis markers in the offshore
511 Mediterranean domain. *CCGM and Memoires de la Societe Geologique de France*, **179**.
512
513 Lofi, J., Gorini, C., Berne, S., Clauzon, G., Dos Reis, A. T., Ryan, W. B. F. & Steckler, M.S. 2005.
514 Erosional processes and paleo-environmental changes in the western Gulf of Lions (SW France)
515 during the Messinian Salinity Crisis. *Marine Geology*, **217** (1–2), 1–30.
516
517 Lugli, S., Manzi, V., Roveri, M. & Schreiber, B.C. 2010. The Primary Lower Gypsum in the
518 Mediterranean: A new facies interpretation for the first stage of the Messinian salinity crisis.
519 *Palaeogeography, Palaeoclimatology, Palaeoecology*, **297**(1), 83–99.
520
521 Lugli, S., Gennari, R., Gvirtzman, Z., Manzi, V., Roveri, M. & Schreiber, B.C. 2013. Evidence of
522 clastic evaporites in the canyons of the Levant Basin (Israel): Implications for the Messinian
523 salinity crisis. *Journal of Sedimentary Research*, **83**(11), 942–954.
524
525 Lugli S., Manzi V., Roveri M. & Schreiber B.C. 2015. The Deep Record of the Messinian salinity
526 crisis: evidence of a non-desiccated Mediterranean Sea. *Palaeogeography, Palaeoclimatology,*
527 *Palaeoecology*, **433**, 201-218.
528
529 Manzi, V., Lugli, S., Ricci Lucchi, F. & Roveri,M. 2005. Deep-water clastic evaporites deposition
530 in theMessinian Adriatic foredeep (northern Apennines, Italy): did theMediterranean ever dry out?
531 *Sedimentology,* **52**, 875–902.

532

533 Manzi, V., Roveri, M., Gennari, R., Bertini, A., Biffi, U., Giunta, S., Iaccarino, S. M., Lanci, L.,
534 Lugli, S., Negri, A., Riva, A., Rossi, M. E. & Taviani, M. 2007. The deep-water counterpart of the
535 Messinian Lower Evaporites in the Apennine foredeep: The Fanantello section (Northern
536 Apennines, Italy). *Palaeogeography, Palaeoclimatology, Palaeoecology*, **251**(3– 4), 470– 499.
537

538 Manzi, V., Lugli, S., Roveri,M. & Schreiber, B.C. 2009. A new facies model for the Upper Gypsum
539 of Sicily (Italy): chronological and paleoenvironmental constraints for the Messinian salinity crisis
540 in the Mediterranean. *Sedimentology*, **56**, 1937–1960.
541

542 Manzi, V., Lugli, S., Roveri,M., Schreiber, B.C. & Gennari, R. 2011. The Messinian "Calcare di
543 Base" (Sicily, Italy) revisited. *Geological Society of America Bulletin, **123**, 347–370.*
544

545 Manzi, V., Gennari, R., Hilgen, F., Krijgsman, W., Lugli, S., Roveri, M. & Sierro, F.J. 2013. Age
546 refinement of the Messinian salinity crisis onset in the Mediterranean. *Terra Nova*, **25**, 315–322.
547

548 Manzi V., Lugli S., Roveri M., Dela Pierre F., Gennari R. Lozar F., Natalicchio M., Schreiber B.C.,
549 Taviani M. & Turco E. 2015. The Messinian salinity crisis in Cyprus: a further step towards a
550 new stratigraphic framework for Eastern Mediterranean. Basin Research, DOI: 10.1111/bre.12107
551

552 Maravelis, A., Panagopoulos, G., Piliotis, I, Pasadakis, N., Manoutsoglou, E. & Zelilidis, A. 2013.
553 Pre-Messinian (Sub-Salt) Source-Rock Potential on Back-Stop Basin of the Hellenic Trench System
554 (Messara Basin, Central Crete, Greece). Oil & Gas Science and Technology, DOI:
555 10.2516/ogst/2013130.
556

557 Maravelis, A.G., Koukonya, A., Tserolas, P., Pasadakis, N. & Zelilidis, N. 2015. Geochemistry of

558 Upper Miocene-Lower Pliocene source rocks in the Hellenic Fold and Thrust Belt, Zakynthos
559 Island, Ionian Sea, western Greece. *Marine and Petroleum Geology*, **66**, 217-230.
560
561 Mezger, E., 2012. How Dry Was the Messinian Salinity Crisis? A Molecular Biogeochemical Study
562 of the Eraclea Minoa (Sicily) Section. (M.Sc. thesis) Utrecht University, Italy 1–34.

563 Ochoa D., Sierro F.J., Lofi J., Maillard A., Flores J.-A. & Suarez M. 2015. Synchronous onset of
564 the Messinian evaporite precipitation: First Mediterranean offshore evidence. Earth and Planetary
565 Science Letters, 427, 112-124.

566 Orszag-Sperber, F., 2006. Changing perspectives in the concept of "Lago-Mare" in Mediterranean
567 Late Miocene evolution. *Sedimentary Geology*, **188–189**, 259–277.

568 Peters, K.E. & Cassa, M.R. 1994. Applied Source Rock Geochemistry. *In*: Magoon, L.E. & Dow,
569 W.G., (eds). The Petroleum system – from source to trap. *Memoir of the American Association of*
570 *Petroleum Geologists*, **60**, 93-129.

571 Rossi, M., Minervini, M., Ghielmi, M. & Rogledi, S. 2015. Messinian and Pliocene erosional
572 surfaces in the Po Plain-Adriatic Basin: Insights from allostratigraphy and sequence stratigraphy in
573 assessing play concepts related to accommodation and gateway turnarounds in tectonically active
574 margins. *Marine and Petroleum Geology*, **66**, 192-216.
575
576 Roveri, M., Boscolo Gallo, A., Rossi, M.E., Gennari, R., Iaccarino, S.M., Lugli, S., Manzi, V.,
577 Negri, A., Rizzini, F. & Taviani, M. 2005. The Adriatic foreland record of Messinian events
578 (central Adriatic Sea, Italy). *Geoacta*, **4**, 139-158.
579
580 Roveri, M. & Manzi, V. 2006. The Messinian salinity crisis: looking for a new paradigm?
581 Palaeogeography, Palaeoclimatology, Palaeoecology, 238, 386–398.

582

583 Roveri, M., Bertini, A., Cosentino, D., Di Stefano, A., Gennari, R., Gliozzi, E., Grossi, F.,
584 Iaccarino, S.M., Lugli, S., Manzi, V. & Taviani, M. 2008a. A high-resolution stratigraphic
585 framework for the latest Messinian events in the Mediterranean area. *Stratigraphy*, **5**, 323–342.
586

587 Roveri, M., Lugli, S., Manzi, V. & Schreiber, B.C. 2008b. The Messinian Sicilian stratigraphy
588 revisited: toward a new scenario for the Messinian salinity crisis. *Terra Nova,* **20**, 483–488.
589

590 Roveri, M., Lugli, S., Manzi, V. & Schreiber, B.C. 2008c. The Messinian salinity crisis: a
591 sequence-stratigraphic approach. *GeoActa Special Publication,* **1**, 169–190.
592

593 Roveri, M., Flecker, R., Krijgsman, W., Lofi, J., Lugli, S., Manzi, V., Sierro, F.J., Bertini, A.,
594 Camerlenghi, A., De Lange, G.J., Govers, R., Hilgen, F.J., Hubscher, C., Meijer, P.T.H. & Stoica,
595 M. 2014a. The Messinian Salinity Crisis: past and future of a great challenge for marine sciences.
596 *Marine Geology*, **352**, 25-58.
597

598 Roveri, M., Manzi, V., Bergamasco, A., Falcieri, F., Gennari, R. & Lugli, S. 2014b. Dense shelf
599 water cascading and Messinian canyons: a new scenario for the Mediterranean salinity crisis.
600 *American Journal of Science*, **314**, 751–784.
601

602 Roveri, M., Lugli, S., Manzi, V., Gennari, R. & Schreiber, B.C. 2014c. High-resolution strontium
603 isotope stratigraphy of the Messinian deep Mediterranean basins: implications for marginal to
604 central basins correlation. *Marine Geology*, **349**, 113–125.
605

606 Ryan, W. B., & Cita, M. B. 1978. The nature and distribution of Messinian erosional surfaces—
607 Indicators of a several-kilometer-deep Mediterranean in the Miocene. *Marine Geology*, **27**, 193-

230.

Ryan, W. B. F. 2009. Decoding the Mediterranean salinity crisis. *Sedimentology,* **56**, 95–136.

Sacleux, M., Nikishin, A., Munch, H., Floodpage, J. & Cornu, T. 2013. Impact of the Messinian Crisis on petroleum systems. American Association of Petroleum Geologists European Regional Conference & Exhibition, Barcelona, Abstract Book, p. 81.

Schmalz, R.F. 1969. Deep-water evaporite deposition, a genetic model. *American Association of Petroleum Geologists Bulletin*, **53**, 798–823.

Sinninghe Damsté, J.S., Frewin, N.L., Kenig, F. & De Leeuw, J.W. 1995. Molecular indicators for palaeoenvironmental change in a Messinian evaporitic sequence (Vena del Gesso, Italy). I: variations in extractable organic matter of ten cyclically deposited marl beds. *Organic Geochemistry*, **23**, 471–483.

Stoica, M., Krijgsman, W., Fortuin, A. & Gliozzi, E. 2016. Paratethyan ostracods in the Spanish Lago-Mare: More evidence for intra-basinal exchange at high Mediterranean sea level. *Palaeogeography, Palaeoclimatology, Palaeoecology*, **441**, 854-870.

Tari, G., Fallah, M., Schell, C., Kosi, W., Bati, Z., Sipahioglu, N.O., Krezseg, Cs., Scheder, Zs., Kozhuharov, E. & Kitchka, A. this volume. Why are there no Messinian evaporites in the Black Sea?

Vai, G.B. 1997. Cyclostratigraphic estimate of the Messinian Stage duration. In: Montanari, A., Odin, G.S., Coccioni, R. (Eds.), Miocene Stratigraphy: An Integrated Approach. *Developments in*

634 *Paleontology and Stratigraphy*, **15**, 463–476.

635

636

637

638

639 **Figure captions**

640

641

642 **Fig. 1.** Chronostratigraphy of the Messinian to Early Pliocene in the Mediterranean basin (modified
643 from Roveri *et al.,* 2014a). MSC events are correlated to the oxygen isotope curve of the Atlantic,
644 to the insolation curve and to the Sr isotope curve.

645

646 **Fig. 2.** Stratigraphic model of the Messinian deep basin deposits and their correlation with marginal
647 basin successions (from Roveri *et al*., 2014c). Note that the "Messinian trilogy" of the western
648 basin would actually almost completely belong to stage 2 and correlate with the salt unit (MU) of
649 the eastern basin. Stage 3 deposits in deep basins would be limited to a very thin unit, with
650 thicknesses usually below normal seismic profiles resolution.

651

652 **Fig. 3.** Source rock potential of Messinian deposits in the different MSC stages. A, map of the
653 central and western Mediterranean showing the provenance of the samples. b-f, S2-TOC plots
654 showing the petroleum potential in particular of pre-MSC and deep stages 1-2 deposits. g-k,
655 modified Van Krevelen diagrams for the different MSC stages. (only including samples with
656 TOC>0,5, and for whom S3 data were available).

657

658 **Fig. 4.** Palynomorph and particulate organic matter distribution in the Messinian successions of the
659 Northern Apennines foreland basin (data from shallow cores). Note the changes in composition in
660 the different MSC stages showing an increase of continental derived organic matter in stage 3.

661

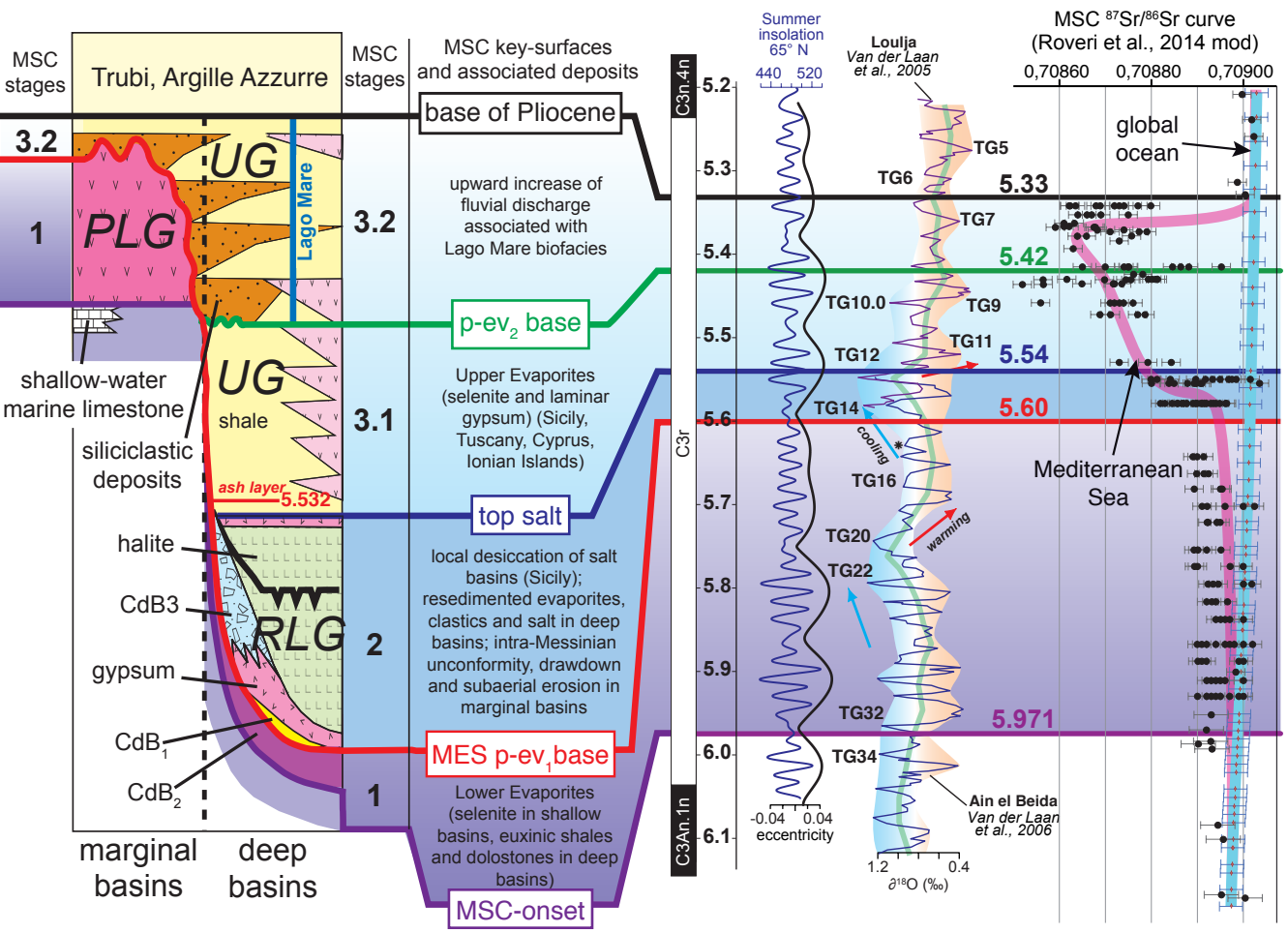
MSC stages
Trubi, Argille Azzurre
MSC stages
MSC key-surfaces and associated deposits
base of Pliocene
3.2
1
PLG
UG
Lago Mare
3.2
upward increase of fluvial discharge associated with Lago Mare biofacies
p-ev2 base
shallow-water marine limestone
UG
shale
3.1
Upper Evaporites (selenite and laminar gypsum) (Sicily, Tuscany, Cyprus, Ionian Islands)
siliciclastic deposits
ash layer
5.532
top salt
halite
CdB3
RLG
2
local desiccation of salt basins (Sicily); resedimented evaporites, clastics and salt in deep basins; intra-Messinian unconformity, drawdown and subaerial erosion in marginal basins
gypsum
CdB1
CdB2
MES p-ev1base
1
Lower Evaporites (selenite in shallow basins, euxinic shales and dolostones in deep basins)
MSC-onset
marginal basins
deep basins
Summer insolation 65° N
440
520
-0.04
0.04
eccentricity
Loulja
Van der Laan et al., 2005
TG5
TG6
TG7
TG10.0
TG9
TG12
TG11
TG14
TG16
TG20
TG22
TG32
TG34
cooling
warming
Ain el Beida
Van der Laan et al., 2006
1.2
0.4
∂18O (‰)
C3n.4n
C3r
C3An.1n
5.2
5.3
5.4
5.5
5.6
5.7
5.8
5.9
6.0
6.1
MSC 87Sr/86Sr curve (Roveri et al., 2014 mod)
0,70860
0,70880
0,70900
global ocean
5.33
5.42
5.54
5.60
5.971
Mediterranean Sea

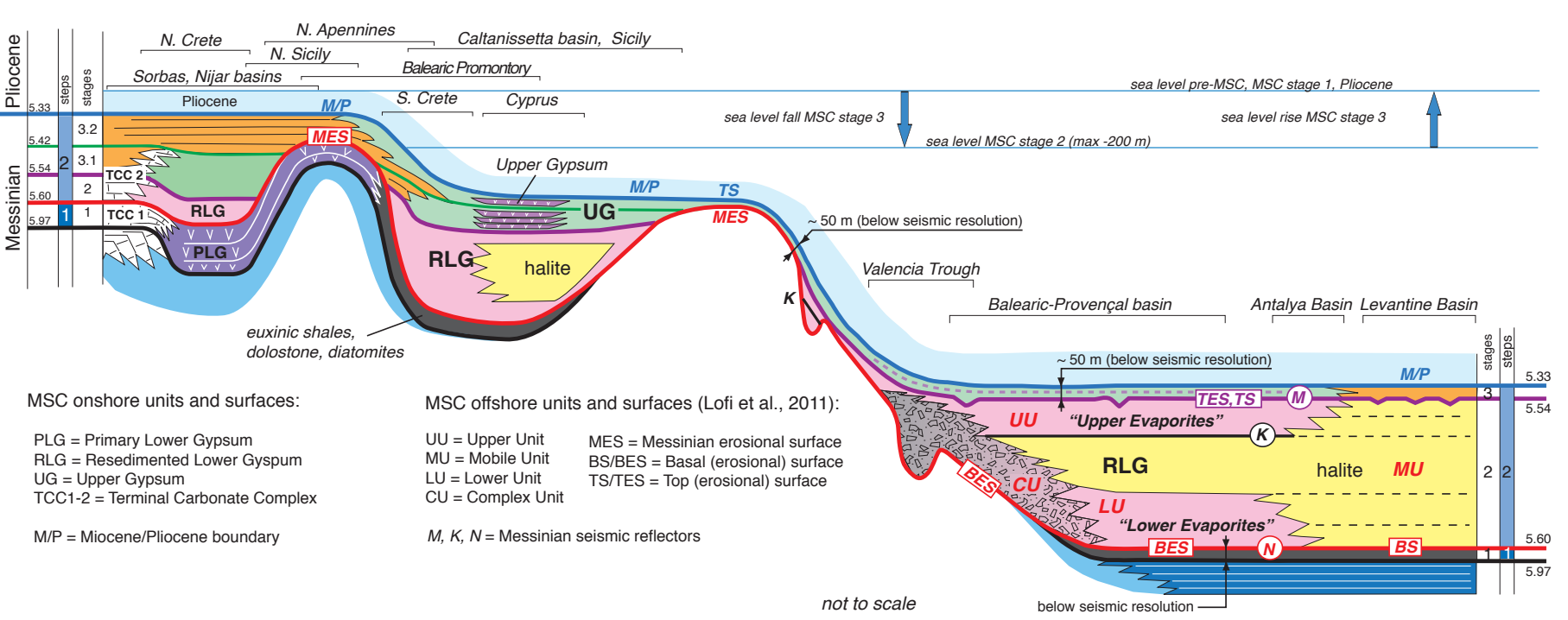

MSC onshore units and surfaces:

PLG = Primary Lower Gypsum
RLG = Resedimented Lower Gyspum
UG = Upper Gypsum
TCC1-2 = Terminal Carbonate Complex

M/P = Miocene/Pliocene boundary

MSC offshore units and surfaces (Lofi et al., 2011):

UU = Upper Unit
MU = Mobile Unit
LU = Lower Unit
CU = Complex Unit

MES = Messinian erosional surface
BS/BES = Basal (erosional) surface
TS/TES = Top (erosional) surface

M, K, N = Messinian seismic reflectors

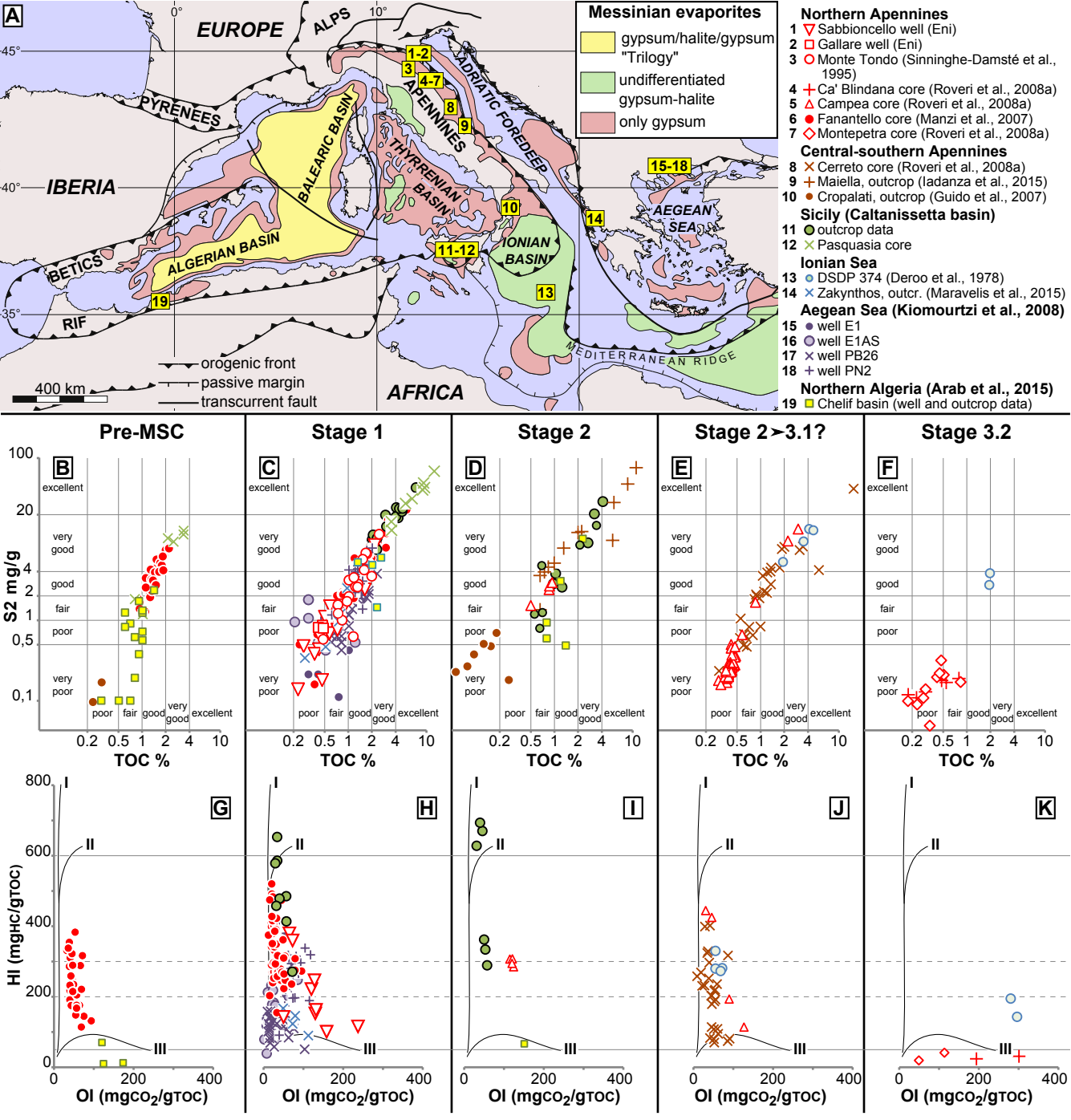
A
EUROPE
ALPS
PYRENEES
IBERIA
BALEARIC BASIN
APENNINES
THYRRENIAN BASIN
ADRIATIC FOREDEEP
ALGERIAN BASIN
BETICS
RIF
IONIAN BASIN
AEGEAN SEA
MEDITERRANEAN RIDGE
AFRICA
1-2
3
4-7
8
9
10
11-12
13
14
15-18
19
0°
10°
45°
40°
35°
400 km
orogenic front
passive margin
transcurrent fault
Messinian evaporites
gypsum/halite/gypsum "Trilogy"
undifferentiated gypsum-halite
only gypsum
Northern Apennines
1 Sabbioncello well (Eni)
2 Gallare well (Eni)
3 Monte Tondo (Sinninghe-Damsté et al., 1995)
4 Ca' Blindana core (Roveri et al., 2008a)
5 Campea core (Roveri et al., 2008a)
6 Fanantello core (Manzi et al., 2007)
7 Montepetra core (Roveri et al., 2008a)
Central-southern Apennines
8 Cerreto core (Roveri et al., 2008a)
9 Maiella, outcrop (Iadanza et al., 2015)
10 Cropalati, outcrop (Guido et al., 2007)
Sicily (Caltanissetta basin)
11 outcrop data
12 Pasquasia core
Ionian Sea
13 DSDP 374 (Deroo et al., 1978)
14 Zakynthos, outcr. (Maravelis et al., 2015)
Aegean Sea (Kiomourtzi et al., 2008)
15 well E1
16 well E1AS
17 well PB26
18 well PN2
Northern Algeria (Arab et al., 2015)
19 Chelif basin (well and outcrop data)
Pre-MSC
Stage 1
Stage 2
Stage 2➢3.1?
Stage 3.2
B
C
D
E
F
excellent
very good
good
fair
poor
very poor
S2 mg/g
100
20
4
2
1
0,5
0,1
poor
fair
good
very good
excellent
0.2
0.5
1
2
4
10
TOC %
G
H
I
J
K
800
600
400
200
0
I
II
III
HI (mgHC/gTOC)
0
200
400
OI (mgCO2/gTOC)

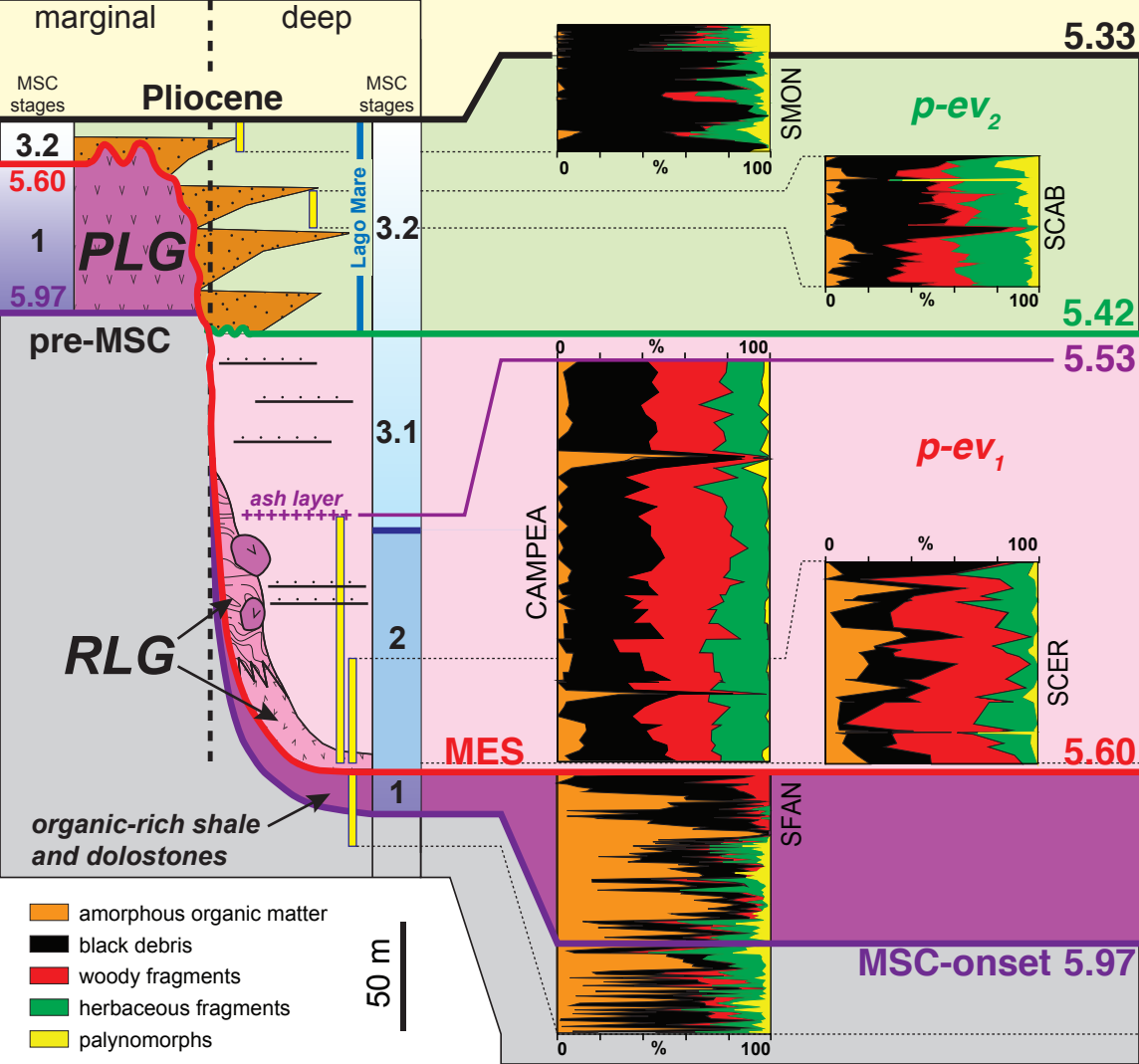
marginal
deep
MSC stages
Pliocene
MSC stages
5.33
3.2
5.60
1
5.97
PLG
Lago Mare
3.2
SMON
p-ev2
SCAB
0
%
100
5.42
pre-MSC
3.1
5.53
p-ev1
ash layer
CAMPEA
SCER
RLG
2
MES
5.60
1
organic-rich shale and dolostones
SFAN
MSC-onset 5.97
amorphous organic matter
black debris
woody fragments
herbaceous fragments
palynomorphs
50 m